Dolaflexin: A Novel Antibody–Drug Conjugate Platform Featuring High Drug Loading and a Controlled Bystander Effect

Aleksandr V. Yurkovetskiy[2], Natalya D. Bodyak[2], Mao Yin[2], Joshua D. Thomas[1], Susan M. Clardy[1], Patrick R. Conlon[2], Cheri A. Stevenson[1], Alex Uttard[1], LiuLiang Qin[1], Dmitry R. Gumerov[2], Elena Ter-Ovanesyan[1], Charlie Bu[2], Alex J. Johnson[2], Venu R. Gurijala[1], Dennis McGillicuddy[2], Michael J. DeVit[2], Laura L. Poling[2], Marina Protopopova[1], Ling Xu, Qingxiu Zhang[1], Peter U. Park[2], Donald A. Bergstrom[2], and Timothy B. Lowinger[1]

ABSTRACT

After significant effort over the last 30 years, antibody–drug conjugates (ADC) have recently gained momentum as a therapeutic modality, and nine ADCs have been approved by the FDA to date, with additional ADCs in late stages of development. Here, we introduce dolaflexin, a novel ADC technology that overcomes key limitations of the most common ADC platforms with two key features: a higher drug-to-antibody ratio and a novel auristatin with a controlled bystander effect. The novel, cell permeable payload, auristatin F-hydroxypropylamide, undergoes metabolic conversion to the highly potent, but less cell permeable auristatin F to balance the bystander effect through drug trapping within target cells. We conducted studies in mice, rats, and cynomolgus monkeys to complement *in vitro* characterization and contrasted the performance of dolaflexin with regard to antitumor activity, pharmacokinetic properties, and safety in comparison with the ADC platform utilized in the approved ADC ado-trastuzumab emtansine (T-DM1). A HER2-targeted dolaflexin ADC was shown to have a much lower threshold of antigen expression for potent cell killing *in vitro*, was effective *in vivo* in tumors with low HER2 expression, and induced tumor regressions in a xenograft model that is resistant to T-DM1.

Introduction

Conceptually, the benefits of an antibody–drug conjugate (ADC) are straightforward: by employing a mAb that specifically recognizes a tumor antigen, accumulation of the conjugated drug in tumor cells can be achieved. In practice, the clinical success of ADCs has been gaining momentum in recent years. Following 30 years of preclinical and clinical research (1), it is widely recognized that the efficacy and tolerability of a given ADC are significantly influenced by the inherent characteristics of the linker-payload platform (2, 3).

One limitation of the majority of ADC platforms is the inability to increase the drug-to-antibody ratio (DAR) beyond values of approximately 3–4. It has been reported with both the maytansines and the auristatins that increased DAR correlates with increased potency *in vitro*; however, efficacy and tolerability *in vivo* are reduced as a result of poor physicochemical and pharmacokinetic properties, such as aggregation and rapid clearance, resulting from the higher drug load (4, 5).

Here, we report on the design and characterization of dolaflexin*, a novel auristatin ADC platform, using a scaffold of poly-1-hydroxymethylethylene hydroxymethylformal, also known as fleximer, together with a novel auristatin drug, auristatin F-hydroxypropylamide (AF-HPA). The high hydrophilicity and polyvalency of the fleximer polymer allow for the preparation of ADCs with DARs of 10–15. These ADCs maintain excellent physicochemical and pharmacokinetic properties and exhibit greater *in vitro* potency and *in vivo* efficacy than ADCs with DARs of 3–4 in tumor xenograft models, including models with low antigen expression. The novel AF-HPA drug payload provides the opportunity for bystander killing, which is beneficial for efficacy in tumors with heterogeneous antigen expression, while eliminating the dose-limiting toxicity of neutropenia commonly observed with the vcMMAE-based auristatin ADC platform (6). Hence, the dolaflexin ADC platform has the potential for an increased therapeutic index.

Materials and Methods

mAbs

Trastuzumab, rituximab, and ado-trastuzumab emtansine (T-DM1) were purchased from Myoderm.

Synthesis of dolaflexin and dolaflexin ADCs

The preparation of dolaflexin is described in the Supplementary Materials and Methods. The preparation of a typical dolaflexin ADC is outlined below, and is represented in **Fig. 1A**, together with the overall

[1]Mersana Therapeutics, Cambridge, Massachusetts. [2]Formerly Mersana Therapeutics, Cambridge, Massachusetts.

Note: Supplementary data for this article are available at Molecular Cancer Therapeutics Online (http://mct.aacrjournals.org/).

Corresponding Author: Timothy B. Lowinger, Mersana Therapeutics, Inc., 840 Memorial Drive, Cambridge, MA 02139. E-mail: tlowinger@mersana.com

Mol Cancer Ther 2021;20:885–95

doi: 10.1158/1535-7163.MCT-20-0166

*The name dolaflexin was chosen as a composite of dolastatin, the natural product class encompassing the auristatins, discovered by Pettit and colleagues (7), and the fleximer polymer.

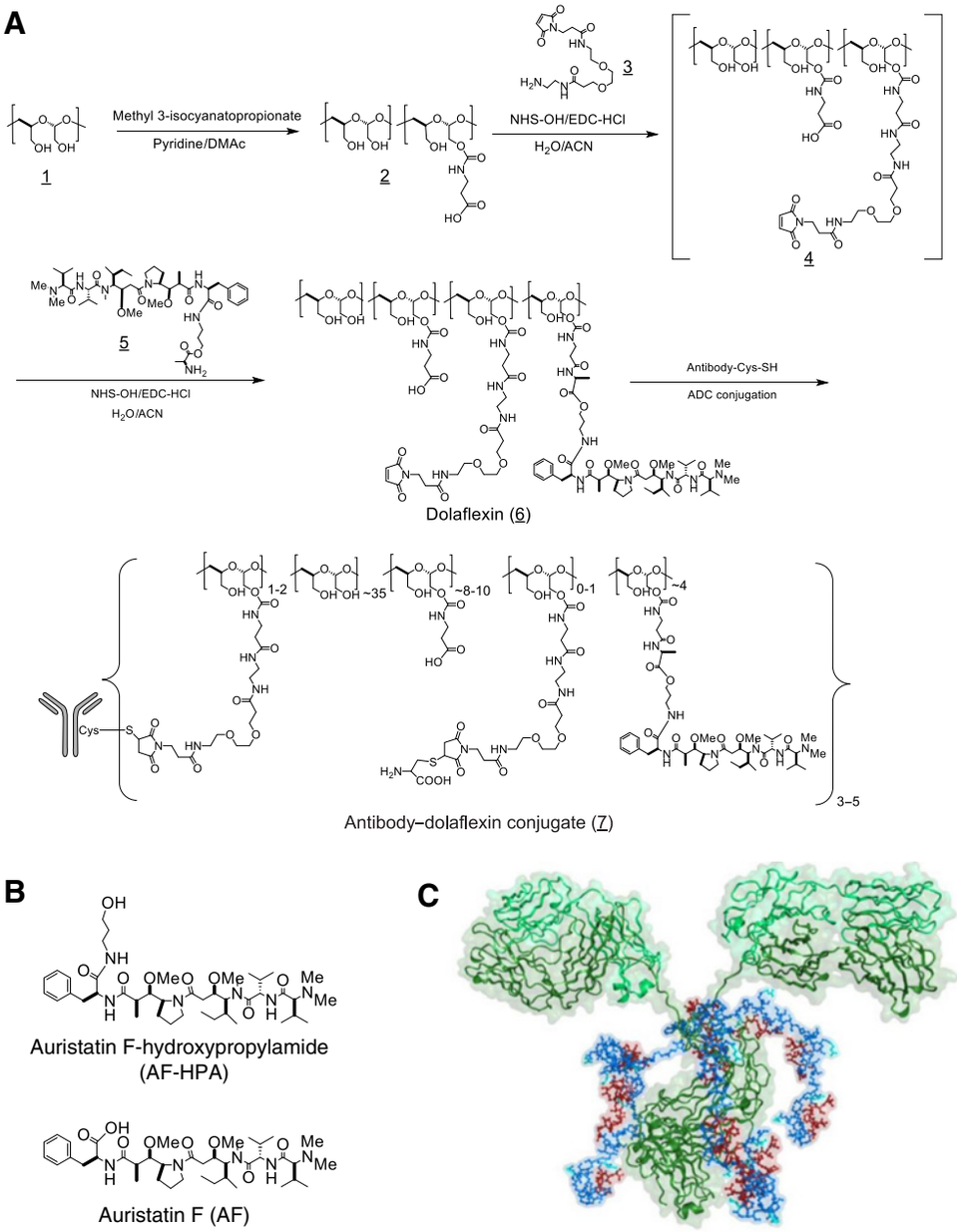

Figure 1.

Synthesis of dolaflexin and dolaflexin ADCs. **A,** Synthetic steps and chemical composition of a dolaflexin ADC. **B,** The small-molecule cytotoxic release products. **C,** A molecular modeling rendition of a dolaflexin ADC; green, antibody; blue, fleximer polymer; red, auristatin F-HPA. The dolaflexin molecules are displayed as bound to cysteines on the heavy chain, however, in practice they are distributed across the eight cysteines that can be generated by reduction of the interchain disulfides of the antibody.

chemical structure. The synthesis and characterization of rituximab-dolaflexin were completed in an analogous manner.

Trastuzumab-dolaflexin (compound 1)

Trastuzumab (400 mg) was diluted with bioconjugation buffer (50 mmol/L triethyl ammonium acetate and 1 mmol/L EDTA, pH 7) to make a 10 mg/mL solution, and 2.18 mg of TCEP (1.21 mL, 1.8 mg/mL, 2.75 equivalents) was added dropwise. The resulting reaction mixture was stirred for 90 minutes. In a separate flask, 191.4 mg (on a dry basis) of dolaflexin (12.76 mL, 15 mg/mL, 7 equivalents) was diluted with 6.38 mL of bioconjugation buffer to make a 10 mg/mL solution, and the pH was adjusted to 7 with 1 N $NaHCO_3$. After 90 minutes, the reduced trastuzumab solution was added by peristaltic pump to the vigorously stirred dolaflexin solution over approximately 15–20 minutes. The reaction mixture was stirred at room temperature for an additional 45 minutes and excess maleimide was quenched by the addition of 99 mg of L-cysteine (10 mL, 10 mg/mL, 50 equivalents). After stirring for an additional 30 minutes, the

reaction mixture was adjusted to pH 5.8 with 1 mol/L acetic acid and filtered through a 0.2 μm filter. The crude ADC was purified by WCX-HPLC (Thermo-Fisher ProPac WCX-10 column; mobile phase A, 20 mmol/L MES and mobile phase B, 20 mmol/L MES and 300 mmol/L NaCl, with gradient 10%–65% B in 32 minutes). Fractions corresponding to the desired product were pooled and concentrated by tangential flow filtration using a 10 kDa MWCO membrane, resulting in trastuzumab-dolaflexin (54% yield; DAR, 12.6).

Analytic methods

Hydrophobic interaction chromatography

Analysis of unconjugated antibody and ADC by hydrophobic interaction chromatography was accomplished by using a TSK-gel Butyl-NPR Column (4.6 mm I.D. × 3.5 cm, 2.5 μm particle size, Tosoh Biosciences) on a Shimadzu Prominence HPLC System. Mobile phase A consisted of 1.5 mol/L ammonium sulfate and 25 mmol/L sodium phosphate, pH 7; and mobile phase B consisted of 22.5 mmol/L sodium phosphate, pH 7 and 10% isopropanol. A total volume of 20 μL of sample diluted to 4 mg/mL with mobile phase A was injected. Separation was achieved using a linear gradient from 100% mobile phase A to 100% mobile phase B over 25 minutes with a flow rate of 1 mL/minute. The column was maintained at 35°C. Monitoring was performed at 280 nm.

Reverse-phase high-performance liquid chromatography

Reverse-phase high-performance liquid chromatography (HPLC) analysis of unconjugated antibody and ADC was carried out on a Shimadzu Prominence HPLC System equipped with a Phenomenex Aeris WIDEPORE XB-C8 Column (4.6 mm I.D. × 250 mm, 3.6 μm particle size, Phenomenex). Mobile phase A consisted of water with 0.1% trifluoroacetic acid (TFA); and mobile phase B consisted of a 1:1 mix of acetonitrile and isopropanol with 0.1% TFA. Prior to injection, the sample was diluted to 1 mg/mL with 50 mmol/L triethylammonium acetate, pH 7, and 1 mmol/L EDTA and reduced at room temperature for 60 minutes with dithiothreitol at a final concentration of 20 mmol/L. A total of 20 μL of this reduced solution was injected with separation performed using a linear gradient from 5% mobile phase B to 60% mobile phase B at 1 mL/minute over 50 minutes at a column temperature of 70°C. Monitoring was performed at 280 nm.

Size-exclusion chromatography

Size-exclusion chromatography was performed on a Shimadzu Prominence HPLC System equipped with a Superose 12 10/300 GL Column (GE Healthcare) held at 30°C. Monitoring was performed at 280 nm. The mobile phase consisted of 50 mmol/L sodium phosphate, pH 7, and 150 mmol/L sodium chloride. A total volume of 20 μL of sample diluted to 2 mg/mL with mobile phase A was injected and chromatographed for 35 minutes at 0.75 mL/minute with monitoring at 280 nm.

Weak cation-exchange chromatography

A Shimadzu Prominence HPLC equipped with a ProPac WCX-10 Column (4 mm I.D. × 250 mm, Thermo Fisher Scientific) was used to compare the charge profiles of trastuzumab and trastuzumab-dolaflexin. Mobile phase A consisted of 20 mmol/L MES, pH 5.8; and mobile phase B consisted of 20 mmol/L MES, pH 5.8, and 300 mmol/L sodium chloride. A total quantity of 80 μg (20 μL, 4 mg/mL) was chromatographed at 35°C using a linear gradient at 1 mL/minute from 10% mobile phase B to 65% mobile phase B over 32 minutes after an initial hold at 10% for 6 minutes. Monitoring was performed at 280 nm.

Capillary isoelectric focusing

The isoelectric points of trastuzumab and trastuzumab-dolaflexin were measured using capillary isoelectric focusing on a PA Plus 800 Pharmaceutical Analysis CE System (Sciex) installed with a Neutral Capillary (50 μm I.D. × 45 cm, Beckman Coulter). The anolyte was 200 mmol/L phosphoric acid and the catholyte was 300 mmol/L sodium hydrazide. Antibody and ADC solutions were desalted and concentrated to a range between 5 and 10 mg/mL. A sample volume of 10 μL was mixed with 240 μL of an ampholyte solution containing Pharmalyte 3-10 (GE Healthcare), 3 mol/L urea in Capillary Isoelectric Focusing Gel (Beckman Coulter), and pI Markers (4.1, 9.5, and 10, Beckman Coulter). Sample-ampholyte mixtures were introduced into the capillary via pressure injection and focused for 15 and 30 minutes at 25 and 30 kV, respectively. Monitoring was performed at 280 nm.

Determination of DAR

The DAR of trastuzumab-dolaflexin was measured by quantitation of AF-HPA released from the ADC after exhaustive hydrolysis. A 1 mg/mL stock solution of ADC in water was diluted 50-fold with 0.5 mol/L sodium phosphate, pH 10.5 and heated at 60°C for 2 hours. A calibration curve for AF-HPA was generated in a similar manner by simultaneous hydrolysis of dolaflexin reference standard solutions ranging from 1,000 to 50,000 ng/mL. The hydrolyzed ADC and dolaflexin standard solutions were precipitated by acidification of 40 μL of sample with 160 μL of 0.1% formic acid in acetonitrile containing isotopically labeled AF-HPA internal standard at 5,000 ng/mL. Following centrifugation to pellet the precipitate, 10 μL of the supernatant was analyzed by LC/MS on an AB Sciex Q3200 Qtrap mass spectrometer. Mass analysis was performed in MRM mode to monitor for AF-HPA (803.5 m/z), AF-HPA internal standard (809.1 m/z), and AF (746.2 m/z). The amount of AF-HPA and AF released from the ADC was quantitated relative to the standard curve generated from dolaflexin hydrolysis and DAR was back-calculated from the original protein concentration of the ADC (1 mg/mL).

Cell culture

Human cancer cell lines were purchased from the ATCC or DSMZ and were cultured according to recommended specifications. All cell lines were maintained in a humidified incubator at 37°C, 5% CO_2. Cell line authentication was performed by short tandem repeat analysis and *Mycoplasma* testing was performed (IDEXX BioAnalytics).

Cell binding

JIMT-1 breast carcinoma cells were grown to approximately 90% confluency and released from the plate surface using Accutase. Cells were then washed once with ice-cold media, resuspended in ice-cold media containing 6% goat serum, seeded at a density of 50,000 cells per well, and incubated on ice for 3 hours with a range of trastuzumab-dolaflexin or trastuzumab concentrations (0.01–500 nM). The cells were washed three times with 100 μL ice-cold PBS, resuspended in 100 μL media with 2% goat serum and 5 μg/mL of Alexa Fluor 647–labeled goat anti-human IgG, and incubated in the dark on ice for 1 hour. The cells were washed three times with 100 μL ice-cold PBS and resuspended in 100 μL of ice-cold PBS with 1% paraformaldehyde. The median fluorescence value for each treatment was determined from 5,000 cells quantified on a MACSQuant Flow Cytometer (Miltenyi Biotec). The Kd value was calculated with GraphPad Prism Software (GraphPad Software Inc.) by nonlinear regression using the one site-specific binding model.

Cell proliferation assay

The CellTiter-Glo Luminescent Cell Viability Assay (Promega) was used to obtain IC_{50} values for test agents. Cells were seeded in 96-well plates (5×10^3 cells/well). Following overnight incubation, cells were treated with the test compounds at various concentrations and incubated continuously for 72 hours (or 144 hours where indicated, due to slower proliferation rate). In the bystander effect experiments, the cells were treated for only 1 hour and then washed before the 72-hour incubation; the IC_{50} values were higher in these experiments on account of the shorter treatment period. IC_{50} values are expressed as nmol/L antibody equivalents and were calculated with GraphPad Prism Software (GraphPad Software Inc.) using 4-parameter, variable slope, dose–response curve fitting algorithm. The methods for the bystander effect studies are described in Supplementary Data.

In vitro metabolism assay for AF-HPA conversion to AF

N87 cells (7E6) in complete media were seeded into 150 mm plates 24 hours prior to performing the assay. On the day of the experiment, media were replaced with 10 mL of 150 nmol/L AF-HPA in fresh media. All timepoints, except t = 0, were then incubated at 37°C for 4 hours for continuous exposure to the drug. The cells were then washed three times with PBS (1×), covered with 10 mL complete media, and returned to 37°C. Media and cells from one plate were collected at the completion of each incubation time (4, 6, 24, and 48 hours). After media retrieval, cells were collected with aid of trypsin (5 mL, 5 minutes, 37°C). Samples were collected and spun down in centrifugation tubes at 1,000 rpm. Tubes containing cell culture media and cell pellets were stored at −80°C until processing for LC/MS analysis.

LC/MS assay for quantitation of AF-HPA and AF *in vitro*

Excess media was removed from the top of cell pellets prior to adding water (100 μL), followed by methanol (200 μL). The sample was then stored at −20°C for 2 hours. After thawing, the sample was mixed and transferred to microtubes prior to adjusting the volume with 50% methanol (to 400 μL). Methanol (200 μL) was added to the thawed media (100 μL). All processed samples (media and cells) were centrifuged at 13,000 rpm for 5 minutes, prior to transferring 60 μL of each processed sample to a 96-well plate. Standards and QCs (30 μL) were also transferred to the same plate and diluted with blank matrix from the control cells (30 μL). An internal standard (60 μL) and 200 mmol/L ammonium acetate (5 μL) were added to all samples prior to centrifuging (15 minutes). The supernatant (10 μL) was then separated on a BEH C4 column during LC/MS analysis.

In vivo studies

All animal studies were performed in compliance with the Animal Welfare Act, the Guide for the Care and Use of Laboratory Animals, and the Office of Laboratory Animal Welfare. Protocols were reviewed and approved by the Institutional Animal Care and Use Committees of the relevant facility.

In vivo efficacy in xenograft models

In vivo efficacy studies were carried out with female 8- to 12-week-old CB.17 SCID mice at Charles River Laboratories. To establish tumors, NCI-N87 or JIMT-1 cells (1×10^7 in 50% Matrigel fragments) were implanted subcutaneously into the flank of each mouse. Tumor size was measured using calipers and tumor volume [$(l \times w^2)/2$] was determined, where l (mm) was the longest and w (mm) was the shortest dimension of the tumor. Tumors were allowed to grow to a target range of 100–150 mm^3, and mice were randomized before treatment was initiated. Mice received a single intravenous bolus injection of ADCs or a dose every 8th day for a total of three doses, as indicated. Mice injected with saline were used as vehicle control. For a partial response (PR), tumor volume had to be 50% or less of its day 1 volume for three consecutive measurements during the course of the study and equal to or greater than 13.5 mm^3 for one or more of these three measurements. For a complete response (CR), tumor volume had to be less than 13.5 mm^3 for three consecutive measurements during the course of the study. A mouse with a CR at the termination of a study was also classified as a tumor-free survivor. To facilitate the comparison of doses relative to ADC dose and payload (toxin) dose, the following values can be used: 1 mg/kg T-DM1 is equivalent to approximately 6.9 nmoles/kg of ado-trastuzumab ADC and approximately 24.1 nmoles/kg of maytansine payload; and 1 mg/kg of trastuzumab-dolaflexin is equivalent to approximately 6.9 nmoles/kg of trastuzumab-dolaflexin ADC and approximately 86.9 nmoles/kg of AF-HPA payload.

Body weight and other toxicity symptoms were monitored. Mice were sacrificed when tumor volume exceeded 800 mm^3 (NCI-N87 models) or 1,000 mm^3 (JIMT-1 model).

Cynomolgus single-dose toxicology

Female cynomolgus monkeys ($n = 4$/group) were administered a single dose of vehicle or trastuzumab-dolaflexin (0.67, 1.34, or 2.68 mg/kg antibody equivalents) via intravenous infusion. Monkeys underwent terminal necropsy on day 3 ($n = 2$) or recovery necropsy on day 22 ($n = 2$). Clinical pathology samples were collected once during acclimation, and on days 3, 8, 15, and 22. Clinical observations were performed twice daily. Body weight was measured once during acclimation on day −1 and once on the day of necropsy. Monkeys that underwent recovery necropsy were also weighed on days 3, 8, and 15.

Mouse single-dose toxicology

Female CD-1 mice ($n = 6$/group) were administered a single intravenous bolus tail vein injection of vehicle or trastuzumab-dolaflexin (20, 30, or 40 mg/kg antibody equivalents). All mice underwent detailed clinical observations and body weight measurement up to day 21.

Rat single-dose toxicology

Female Sprague Dawley rats ($n = 6$/group) were administered a single intravenous bolus tail vein injection of vehicle or trastuzumab-dolaflexin (2.5, 5, or 10 mg/kg antibody equivalents). All rats underwent detailed clinical observations and body weight measurement up to day 21.

Pharmacokinetics analysis of trastuzumab-dolaflexin

Mouse pharmacokinetics study

Female CD-1 mice were injected intravenously with 3 mg/kg of trastuzumab-dolaflexin or T-DM1. To assess circulating levels of total antibody, total drug, free AF-HPA, and free AF, blood was collected from three mice via cardiac puncture into prechilled lithium heparin tubes at the following timepoints: 5 minutes and 1 hour, 6 hours, 24 hours, 48 hours, 72 hours, 168 hours, 336 hours, 504 hours, and 672 hours post injection. Blood was processed for plasma within 30 minutes of collection.

Cynomolgus monkey pharmacokinetics study

Female cynomolgus monkeys were administered a 1-hour (±10 minutes) intravenous infusion of trastuzumab-dolaflexin via a peripheral vein using a pump at the following doses: 0.67, 1.34, or 2.68 mg/kg.

Blood samples were collected before infusions, and then 10 minutes and 1 hour, 6 hours, 24 hours, 48 hours, 72 hours, 96 hours, 192 hours, 360 hours, and 528 hours post infusion. Four monkeys were used for blood collections from 10 minutes to 48 hours, and two monkeys were used thereafter. Blood samples, approximately 0.5 mL, were collected in prechilled lithium heparin tubes and processed for plasma within 30 minutes.

Quantitation of total antibody in plasma samples

Total trastuzumab concentration in plasma samples was measured as follows: 96-well ELISA plates were coated with 1 μg/mL recombinant ECD in 50 mmol/L carbonate/bicarbonate buffer, pH 9 for 2 hours at room temperature, washed four times with TBST, and blocked with 3% BSA in TBST for 1 hour at room temperature. Plates were washed four times with TBST. Plasma samples or standards were diluted in TBST with 3% BSA and protease inhibitors and added to plates either in triplicate (samples) or duplicate (standards), and then incubated for 2 hours at room temperature. Plates were then washed and incubated with anti-human IgG-HRP secondary antibody for 1 hour at room temperature. Plates were washed again, and then tetramethyl benzidine substrate was added for color development. The reaction was stopped by the addition of 0.2 N sulfuric acid.

Quantitation of free AF-HPA and free AF in plasma samples

Free AF-HPA and AF in plasma were quantitated by LC/MS. The unconjugated auristatin payloads were extracted by addition of 0.1% formic acid in acetonitrile containing 30 ng/mL of auristatin E to plasma samples in a 4:1 ratio. Samples were mixed for 5 minutes, followed by centrifugation at 13,000 × *g* for 15 minutes. A 10-μL injection volume was used to conduct LC/MS analysis. Quantitation of AF-HPA and AF was based on standard curves of each analyte ranging from 0.5 to 1,000 ng/mL.

Quantification of total drug in plasma samples

Total drug present in plasma was determined by base-mediated hydrolysis of the ester in the ADC, resulting in the liberation of AF-HPA, which was quantified by LC/MS. Plasma samples (40 μL) were incubated with 1 N NaOH (10 μL) for 2 hours at 60°C. The decoupled AF-HPA payload was extracted by addition of 2.5% formic acid in acetonitrile containing 100 ng/mL of auristatin E in a 4:1 ratio. Samples were mixed for 5 minutes, followed by centrifugation at 13,000 × *g* for 15 minutes. A 10-μL injection volume was used to conduct LC/MS analysis. Quantitation of AF-HPA was based on a standard curve ranging from 1 to 10,000 ng/mL.

Statistical analysis

For *in vivo* xenograft experiments, statistical analysis was performed by the log-rank and Mann–Whitney tests using Prism v3.03 (GraphPad Software).

Results

Trastuzumab-dolaflexin

The structure of trastuzumab-dolaflexin is shown in **Fig. 1A**. Dolaflexin is a polymer that incorporates multiple monomers of distinct structures. The average relative amounts of each monomer are reproducible and controlled by the stoichiometry of the reactions, as well as chromatographic purifications of the intermediates and final material. On average, each dolaflexin polymer conjugated to an antibody consisted of the following relative number of monomers: approximately 1–2 monomers containing a maleimide moiety conjugated to the antibody via cysteine residues; approximately 35 unsubstituted monomers, which are highly hydrophilic by nature of the hydroxyl groups and acetal backbone; approximately 8–10 monomers that incorporate a β-alanine moiety, are negatively charged at physiologic pH, and contribute to hydrophilicity; approximately 0–1 monomers in which the maleimide moiety did not undergo bioconjugation with the antibody and was capped as the cysteine adduct; and approximately four monomers that incorporate an AF-HPA payload covalently attached to the polymer backbone via a linker containing an ester functionality. The two alcohols within each monomer are not equivalent and, in practice, either alcohol can be functionalized; for clarity, only one of the two alcohols is shown as substituted in **Fig. 1A**. The DAR of the ADC was controlled by partial reduction of interchain disulfides within the antibody to limit the number of reactive cysteines generated; a typical DAR of 10–15 incorporates an average of 3–5 dolaflexin polymers per antibody. The ester moiety between the AF-HPA payload and the polymer was highly stable in plasma (Supplementary Table S2) and is readily cleaved upon internalization to release the cell permeable payload AF-HPA (**Fig. 1B**). AF-HPA can be further metabolized by amidolysis to the carboxylate-containing species AF (**Fig. 1B**), which has reduced cell permeability associated with its greater hydrophilicity and negative charge. The logD values as a function of pH were calculated (ChemAxon software) for AF-HPA and AF and were found to be similar to those for the well-known auristatins MMAE and MMAF, respectively (Supplementary Fig. S1). AF-HPA was found to be a substrate for Pgp efflux pumps, whereas AF was not (Supplementary Table S3). A molecular model of trastuzumab-dolaflexin is shown in **Fig. 1C**. For clarity, the dolaflexin molecules are shown conjugated to cysteines in the heavy chain, but in principle they are conjugated stochastically to any of the cysteines generated from reduction of interchain disulfides.

Physicochemical characterization

Analysis by hydrophobic interaction chromatography (**Fig. 2A**) shows an increase in hydrophobicity of the ADC relative to the unconjugated antibody based on elution time, consistent with the incorporation of multiple molecules of the highly hydrophobic AF-HPA payload. The ADC was extensively conjugated, as unconjugated antibody was negligible in the final product. A high degree of conjugation was also seen in reverse-phase HPLC after reduction (**Fig. 2B**), where the majority of species observed were more hydrophobic than the constituent light and heavy chains of the antibody alone. Trastuzumab-dolaflexin was primarily monomeric, as determined by size-exclusion chromatography (**Fig. 2C**), with aggregation levels below 5%; this was also confirmed by analytic ultracentrifugation (method provided in Supplementary Data). The effect of conjugating dolaflexin on the charge profile of trastuzumab can be seen by cation-exchange chromatography (**Fig. 2D**), with decreased elution time for the ADC, suggesting a more negatively charged state relative to the antibody. This result was consistent with the decreased pI of the ADC, as observed by capillary isoelectric focusing (**Fig. 2E**), and was consistent with the incorporation of dolaflexin, which contains negatively charged carboxylate residues along the polymer backbone. Conjugation of the antibody resulted in the conversion of the five antibody peaks around pI 8.53 to a large collection of peaks with lower pI around 7.48.

Trastuzumab-dolaflexin exhibits potent *in vitro* cytotoxicity

The binding of trastuzumab-dolaflexin was comparable with that of unconjugated trastuzumab across a broad range of antibody concentrations. Using an ELISA method (**Fig. 3A**), nonlinear

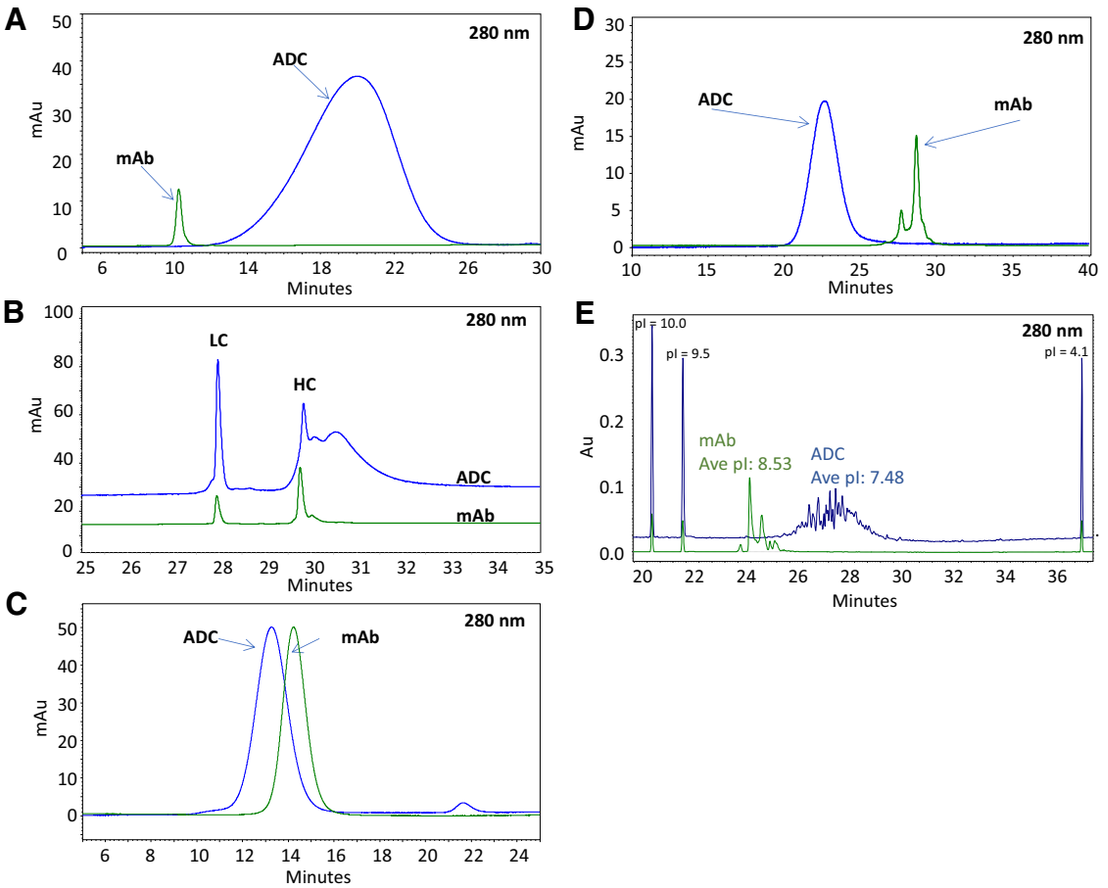

Figure 2.

Physicochemical characterization of trastuzumab-dolaflexin. **A,** Overlay of hydrophobic interaction chromatography chromatograms of trastuzumab-dolaflexin (blue) and unconjugated trastuzumab (green). **B,** Overlay of reverse-phase HPLC chromatograms of trastuzumab-dolaflexin (blue) and unconjugated trastuzumab (green). **C,** Overlay of size-exclusion chromatograms of trastuzumab-dolaflexin (blue) and unconjugated trastuzumab (green). **D,** Overlay of weak cation-exchange chromatograms of trastuzumab-dolaflexin (blue) and unconjugated trastuzumab (green). **E,** Overlay of capillary isoelectric focusing electropherograms of trastuzumab-dolaflexin (blue) and unconjugated trastuzumab (green).

regression analysis indicated comparable binding affinities (EC_{50}) of 0.014 nM for trastuzumab-dolaflexin and 0.010 nM for trastuzumab. As expected, rituximab did not exhibit any binding, which confirmed assay specificity.

Similarly, trastuzumab-dolaflexin and unconjugated trastuzumab also exhibited comparable binding to JIMT-1 breast cancer cells, which express endogenous HER2, based on flow cytometry (**Fig. 3B**). Nonlinear regression analysis indicated comparable binding affinities (EC_{50}) of 5.4 nM for trastuzumab-dolaflexin and 3.5 nM for trastuzumab.

The cytotoxicity of trastuzumab-dolaflexin in comparison with that for T-DM1 was measured in 31 cancer cell lines established from breast, gastric, lung, and ovarian cancers (**Fig. 3C**). An IC_{50} value of 1 nM or less was achieved in all breast cancer cell lines with at least 30,000 receptors, except one, and in all lung cancer cell lines with at least 10,000 receptors, except one. Three gastric cancer cell lines with approximately 20,000 HER2 receptors had similar IC_{50} values of approximately 10 nM, whereas NCI-N87 cells had an IC_{50} value of approximately 0.03 nM, likely due to the higher receptor number (~870,000). Cell line names and IC_{50} values are shown in Supplementary Table S1. Trastuzumab-dolaflexin was more potent than T-DM1 in all cell lines tested (**Fig. 3C**). The broad range of fold difference values (Supplementary Table S1) could reflect the different linkers and toxins present in T-DM1 and trastuzumab-dolaflexin (as opposed to simply higher DAR), which could be processed differently among cell types. The cytotoxicity of trastuzumab-dolaflexin was found to be target dependent, as the control dolaflexin ADC (rituximab-dolaflexin) that did not bind the target cells was typically approximately 1,000-fold less potent than trastuzumab-dolaflexin (Supplementary Fig. S4).

Efficacy of trastuzumab-dolaflexin ADCs in a xenograft model of human gastric cancer

HER2-amplified NCI-N87 human gastric cancer xenograft tumor–bearing mice were treated once with vehicle (saline control), T-DM1 (10/0.17 mg/kg antibody equivalents/DM1 equivalents), or trastuzumab-dolaflexin (1/0.065 and 3/0.20 mg/kg antibody/AF-HPA equivalents). As a control, mice were treated with a nonbinding IgG1-dolaflexin ADC (3/0.27 mg/kg antibody/AF-HPA equivalents), which was administered every 8th day for a total of three doses. Trastuzumab-dolaflexin (**Fig. 4A**) exhibited the greatest efficacy, with a 100% regression response rate (10 CRs that were also tumor-free survivors

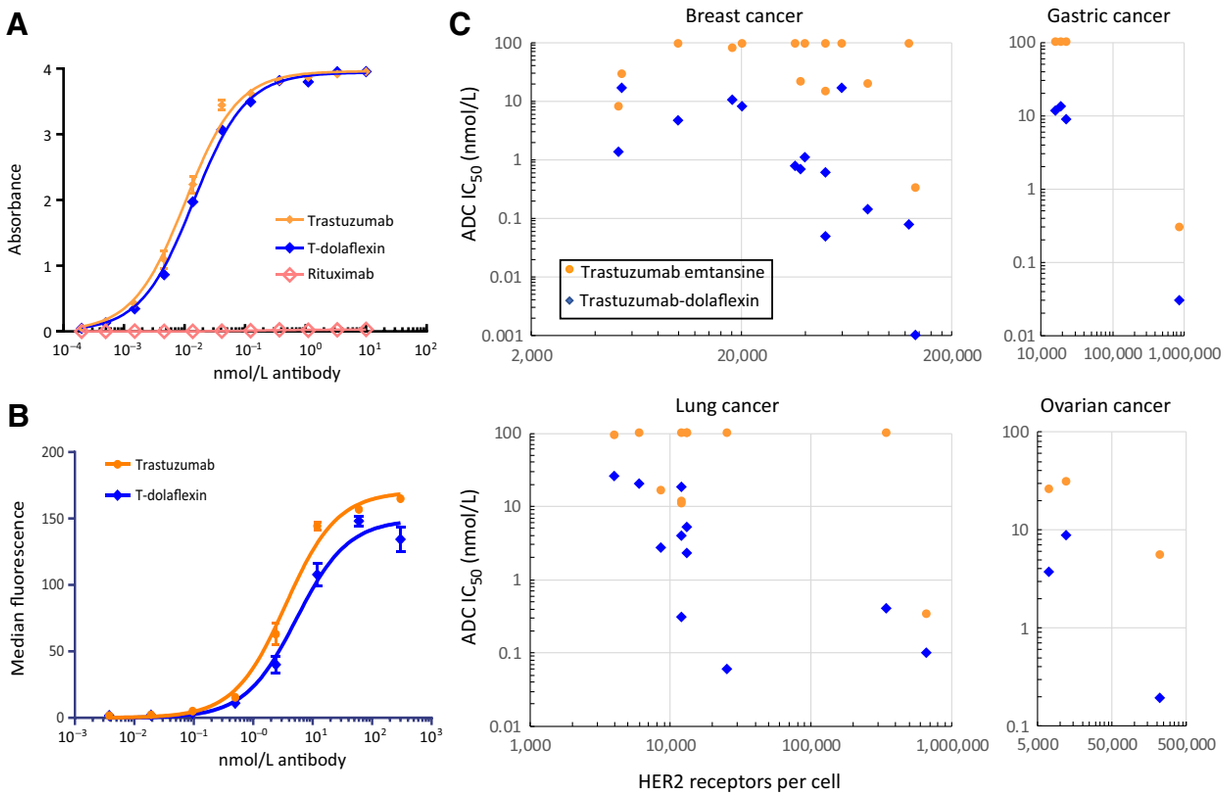

Figure 3.

In vitro characterization of trastuzumab (T)-dolaflexin conjugate. **A,** Trastuzumab-dolaflexin ADC (blue diamonds) and unconjugated trastuzumab (orange diamonds) exhibited comparable binding to recombinant HER2 antigen. Binding was measured for a series of antibody concentrations using ELISA. Rituximab (pink open diamonds) served as a negative control, and no binding was observed. Error bars indicate SEM. **B,** Trastuzumab-dolaflexin ADC (blue diamonds) and unconjugated trastuzumab (orange diamonds) exhibited comparable binding to cancer cells. Binding to JIMT-1 breast cancer cells was measured for a series of antibody concentrations by flow cytometry. Error bars indicate SEM. **C,** Cytotoxicity of trastuzumab-dolaflexin (blue diamonds) and T-DM1 (orange circles) against cancer cell lines representing breast, gastric, lung, and ovarian cancers. Cell lines with HER2 amplification are indicated by symbols with black border. HER2 receptor numbers and IC_{50} values were determined as explained in the Materials and Methods section.

on day 75). Trastuzumab-dolaflexin administered at a single 1 mg/kg dose was also active, resulting in 80% regressions that included seven PRs and one CR. Both doses had significant survival benefit compared with vehicle ($P < 0.001$, log-rank test) and were well-tolerated, with maximum mean body weight loss within acceptable limits for all groups. Clinical observations were unremarkable. Treatment with T-DM1 resulted in 100% regressions, consisting of four PRs and five CRs, one of which remained a tumor-free survivor on day 75. The nonbinding control IgG1-dolaflexin group had no regressions and slight tumor growth delay.

Efficacy of trastuzumab-dolaflexin ADCs in a xenograft model of human breast cancer

The *in vivo* antitumor activity of trastuzumab-dolaflexin ADCs was further evaluated in the HER2 (2+) JIMT-1 human breast cancer xenograft model, which has been shown to be intrinsically resistant to T-DM1 (**Fig. 4B**; ref. 8). Tumor-bearing mice were administered a single dose of vehicle (saline control), T-DM1 [20/0.34 mg/kg (antibody equivalents/DM1 equivalents)], trastuzumab-dolaflexin (0.3/0.019, 0.67/0.043, and 2/0.13 mg/kg antibody equivalents/AF-HPA equivalents), or nonbinding control rituximab-dolaflexin (2/0.17 mg/kg antibody equivalents/AF-HPA equivalents). Trastuzumab-dolaflexin was the only active agent in this model. Treatment with 2 mg/kg resulted in a 100% regression response rate (10 CRs that were also tumor-free survivors on day 69). The 0.67 mg/kg trastuzumab-dolaflexin dose resulted in four of 10 PRs. Both doses produced tumor growth inhibition that differed statistically from vehicle control ($P < 0.001$, Mann–Whitney test). T-DM1 administered at a 10-fold higher antibody dose than trastuzumab-dolaflexin (20 mg/kg) did not produce any regressions, but overall survival differed significantly from vehicle control ($P < 0.05$, log-rank test). Non-binding control rituximab-dolaflexin administered at 2 mg/kg antibody dose was not active and did not differ statistically from vehicle control ($P < 0.05$, Mann–Whitney test).

MTD and pharmacokinetics of trastuzumab-dolaflexin ADC in mice

Female CD-1 mice were treated with a single dose of vehicle or trastuzumab-dolaflexin (20, 30, and 40 mg/kg antibody equivalents). At the highest dose of 40 mg/kg, 1 mouse was found dead and another became moribund and was euthanized on day 17. All other mice on the study survived. Average body weight loss was dose proportional and reached the lowest value between days 5 and 9 (**Fig. 5A**). On the basis of gross tolerability and body weight loss, the MTD was concluded to be 30 mg/kg.

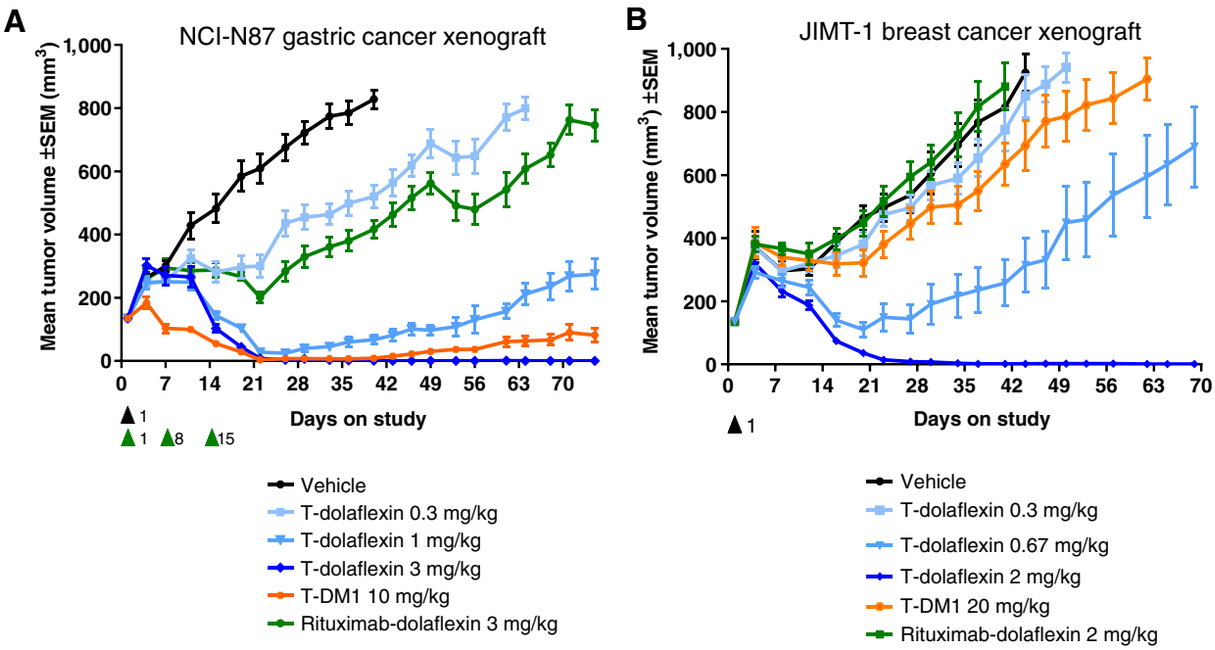

Figure 4.

In vivo efficacy of trastuzumab-dolaflexin. **A,** Tumor growth curves of NCI-N87 gastric cancer xenografts in CB17.scid mice. Animals were intravenously administered a single dose of vehicle, trastuzumab (T)-dolaflexin, or T-DM1, or three doses of control ADC (rituximab-dolaflexin) on the days indicated. Tumor volumes are shown as mean with SEM. **B,** Tumor growth curves of JIMT-1 breast cancer xenografts in CB17.scid mice. Animals were intravenously administered a single dose of vehicle, trastuzumab-dolaflexin, T-DM1, or control ADC (rituximab-dolaflexin). Tumor volumes are shown as mean with SEM.

After a single intravenous dose of either T-DM1 or trastuzumab-dolaflexin at 3 mg/kg in mice, comparable total antibody pharmacokinetic profiles were observed between these two groups, with a $t_{1/2}$ for total antibody of 10–15 days (representative data are presented in **Fig. 5B**). The small-molecule release products, free AF-HPA and free AF, were not detectable (below limit of quantitation), suggesting little to no deconjugation of the drug from the ADC.

MTD of trastuzumab-dolaflexin ADCs in rats

Female Sprague Dawley rats were treated with a single dose of vehicle or trastuzumab-dolaflexin (2.5, 5, and 10 mg/kg antibody equivalents). At the highest dose of 10 mg/kg, hind paw swelling with limb disuse was noted in 1 rat on day 13. This observation resulted in unscheduled euthanasia. All other rats in the study survived. Average body weight loss was dose proportional and reached nadirs on day 4 (**Fig. 5C**). The MTD was considered to be 5 mg/kg.

Tolerability and pharmacokinetics of trastuzumab-dolaflexin ADCs in cynomolgus monkeys

All cynomolgus monkeys treated with a single dose of vehicle or trastuzumab-dolaflexin (0.67, 1.34, and 2.68 mg/kg antibody equivalents) survived until scheduled necropsy with limited body weight loss. There were no test article–related findings on gross pathology. The most notable clinical pathology findings at the 2.68 mg/kg dose level were transient transaminase elevations (primarily aspartate aminotransferase), which peaked at day 8 and normalized by day 22, and moderately decreased platelet counts at day 8, which returned to normal by day 15. No test article–related findings were observed in HER2-expressing organs, including heart, lungs, and gastrointestinal tract. Neutrophils were slightly increased in all treatment groups (**Fig. 5D**), most notably on day 3, with no evidence of neutropenia at any timepoint or dose level.

After a single dose of trastuzumab-dolaflexin in monkey, total antibody and conjugated AF-HPA showed an approximately dose proportional increase of exposure (C_{max} or AUC). Linear pharmacokinetics were suggested by similar clearances among the three tested dose levels for both total antibody and total AF-HPA (Supplementary Fig. S2). Free (unconjugated) AF-HPA and AF concentrations were low (less than 2 ng/mL) at all doses tested (representative data for the 2.68 mg/kg dose are presented in **Fig. 5E**).

Dolaflexin exerts a novel controlled bystander effect

Because fleximer polymer ester linkages have been shown to be highly stable in circulation and readily cleaved upon cell internalization (9), we sought to identify a suitable auristatin derivative that could be linked via an ester. We prepared and evaluated a number of novel auristatin derivatives for *in vitro* potency, physicochemical properties, and metabolic stability. Over the course of this effort, we identified the novel derivative, AF-HPA [**Fig. 6A** (i)]. This molecule contains an alcohol moiety, thereby allowing facile incorporation into the polymer–drug conjugate via an ester linkage, and was found to be highly potent and capable of bystander killing. Moreover, we observed that AF-HPA could be readily metabolized to the corresponding carboxylate derivate AF [**Fig. 6A** (ii)] in tumor cells.

We hypothesized that the membrane permeability of AF-HPA would enable the "bystander effect" by which antigen-negative cells are indirectly killed by the migration of payload released in neighboring antigen-positive cells. The intracellular conversion of AF-HPA to nonpermeable AF would trap payload in the tumor cells and prevent the undesired escape of toxin beyond the tumor, as well as prevent the

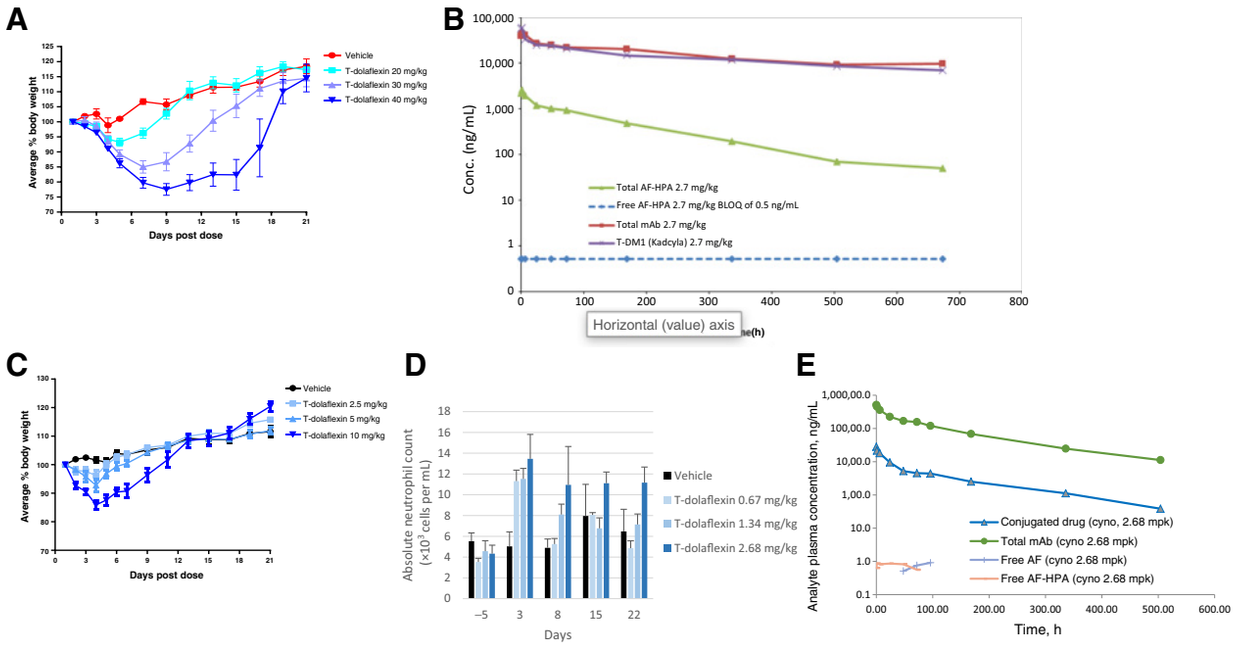

Figure 5.

Tolerability and pharmacokinetic profile of trastuzumab (T)-dolaflexin. **A,** Body weights of female CD-1 mice following a single intravenous administration of trastuzumab-dolaflexin. All mice survived, except for two animals in the 40 mg/kg group; thus the MTD was determined to be 30 mg/kg. **B,** Plasma concentrations of total antibody, conjugated drug, and free drug in mice following a single intravenous administration of trastuzumab-dolaflexin or T-DM1 at 3 mg/kg antibody dose (conjugated and free-drug analytes were not studied for T-DM1). **C,** Body weights of Sprague Dawley rats following a single intravenous administration of trastuzumab-dolaflexin. All rats survived, except for one animal in the 10 mg/kg group; thus the MTD was determined to be 5 mg/kg. **D,** Neutrophil counts of cynomolgus monkeys following a single intravenous administration of trastuzumab-dolaflexin. **E,** Pharmacokinetics profile of trastuzumab-dolaflexin in cynomolgus monkeys following a single intravenous administration at 2.68 mg/kg by antibody.

passive distribution of the metabolite AF toxin to healthy cells after tumor lysis.

We first confirmed that both payload forms are formed and can be detected in cells upon incubation with trastuzumab-dolaflexin. As shown in **Fig. 6B**, exposure of N87 cells to trastuzumab-dolaflexin results in the formation of both payloads within the cell, with rapid accumulation of the cell permeable AF-HPA and slow conversion to the relatively cell impermeable metabolite, AF. We further confirmed that both AF-HPA and AF were observed in tumors 48 hours after mice were injected with trastuzumab-dolaflexin. Tumors and several normal tissues were harvested and processed, and samples were analyzed by mass spectrometry. Significant quantities of both AF-HPA and AF were detected in tumors, and to a substantially lower degree in some normal tissues (**Fig. 6C**). This result demonstrated that the dolaflexin-based ADC dosed *in vivo* yielded two auristatins with distinct, complementary biophysical properties.

We also tested the two auristatins for *in vitro* potency against a panel of cancer cell lines. Consistent with the prediction that AF is less membrane permeable and would be less effective in this cell-based assay, AF-HPA was more potent than AF in every cell line tested by an average of 8.3-fold (**Fig. 6D**). This is notable because previous findings suggest that AF inhibits tubulin polymerization with a potency comparable with that of its methyl ester membrane permeable derivative (10); thus, AF that is produced within the target cell should have potency similar to (or even greater than, **Fig. 6D**) that of AF-HPA.

To test our hypothesis that dolaflexin-based ADCs would exhibit bystander effect, we devised a coculture system with HER2-negative MDA-MB-231 cells expressing red fluorescence protein and HER2-positive NCI-N87 cells expressing GFP. Cell lines were treated with trastuzumab-dolaflexin alone or in coculture (3:1 ratio of NCI-N87: MDA-MB-231); see Supplementary Data for detailed methods. As expected, trastuzumab-dolaflexin efficiently killed the Her2-positive NCI-N87 cells regardless of the presence of MDA-MB-231 cells (Supplementary Fig. S3C). Trastuzumab-dolaflexin did not kill MDA-MB-231 cells when cultured alone, as expected; but strikingly, trastuzumab-dolaflexin killed MDA-MB-231 cells when they were cultured with NCI-N87 cells, with $IC_{50} = 6.5$ nM (**Fig. 6E** and **F**; Supplementary Fig. S3A). The nonbinding control ADC did not elicit any appreciable cytotoxic effect in this system (Supplementary Fig. S3B). Each of the bystander effect experiments (including control treatments) was conducted at least three times, and the results were comparable. Taken together, these data indicate that MDA-MB-231 cells were indirectly killed by a bystander effect via the antigen-positive cells

Discussion

Dolaflexin is a novel ADC platform with a high DAR and a controlled bystander effect, and provides excellent preclinical efficacy and tolerability.

High drug loading will lead to increased cytotoxic effects, but when this is accomplished using conventional technologies it is at the expense of physicochemical properties. For both the established maytansine (4) and vcMMAE auristatin (5) ADC platforms, *in vitro* potency increases with increasing DAR. However, *in vivo* efficacy decreases significantly for ADCs with a DAR above

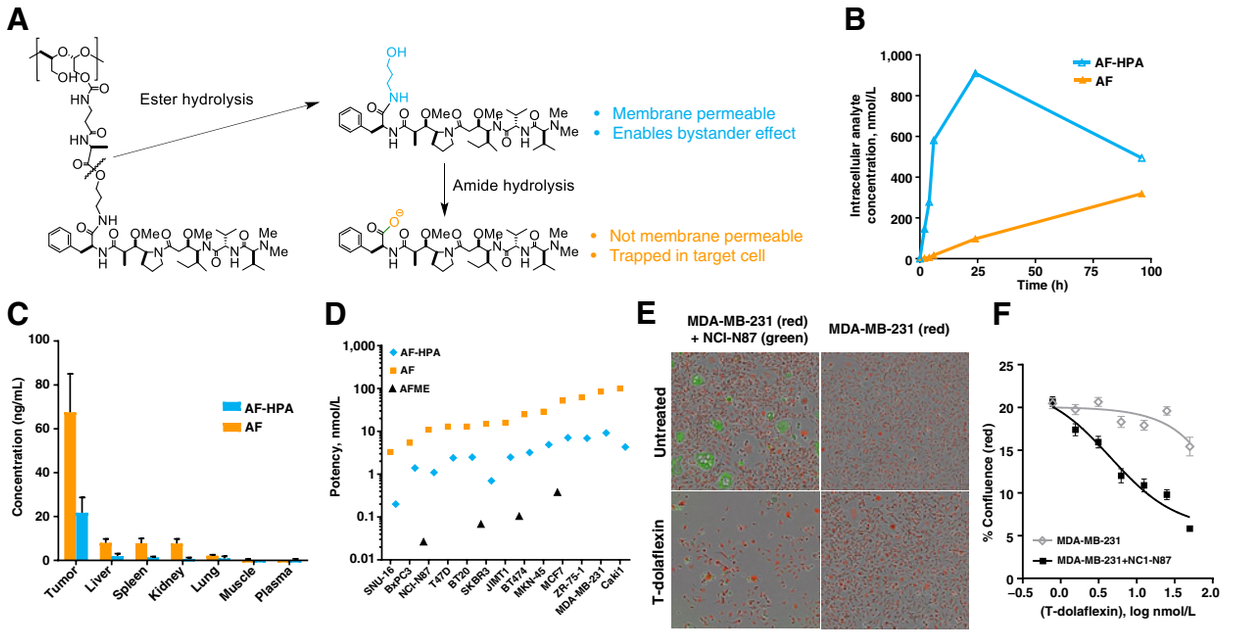

Figure 6.

Dolaflexin yields two auristatin variants and demonstrates a controlled bystander effect. **A,** Schematic of the production of two variants of auristatin from dolaflexin. Ester hydrolysis yields AF-HPA, which is membrane permeable. Within the target cell, AF-HPA can be converted into the negatively charged and less cell permeable AF by amide hydrolysis. **B,** Quantitation of AF-HPA and AF over time after exposure of N87 cells to trastuzumab-dolaflexin. **C,** Both AF and AF-HPA were observed in NCI-N87 tumor mouse xenografts after one administration of trastuzumab (T)-dolaflexin. Tumors and several normal tissues were harvested 48 hours after intravenous injection of 0.67 mg/kg trastuzumab-dolaflexin. Tissues were processed and AF-HPA and AF were quantitated. **D,** *In vitro* potency of AF (orange squares) and AF-HPA (blue diamonds) and the cell permeable AF methyl ester (black triangles) across a panel of cancer cell lines. **E** and **F,** HER2-negative MDA-MB-231 cells (red) were not directly killed by trastuzumab-dolaflexin, but were indirectly killed in the presence of HER2-positive NCI-N87 cells (green). NCI-N87 cells were plated in a 3:1 ratio to MDA-MB-231 cells in the coculture. **E,** Micrographs demonstrate the effect of 25 nM trastuzumab-dolaflexin. **F,** Measurements were of confluency of red color, with error bars indicating SEM. Detailed methods and additional controls are provided in Supplementary Data.

approximately 4. Recently, it has been shown that the use of hydrophilic linkers to compensate for payload hydrophobicity allows for the preparation of auristatin ADCs with a DAR of up to 8. The *in vitro* and *in vivo* efficacies of these ADCs were superior to that of ADCs with a DAR of 4 (11).

We reported previously the application of a highly hydrophilic, biodegradable polymer (fleximer) in an antibody-vinca drug conjugation platform, allowing for the preparation of ADCs with a DAR of 20 that maintained excellent physicochemical and pharmacokinetic properties and displayed *in vivo* efficacy (9). In this study, we have extended the use of fleximer to create dolaflexin, which incorporates a novel auristatin analogue.

The threshold of antigen expression needed to achieve effective cell killing with trastuzumab-dolaflexin was lower than that for T-DM1 in both *in vitro* and *in vivo* systems. Trastuzumab-dolaflexin demonstrated a cytotoxic effect in cell lines with target expression levels significantly lower than those lines where a cytotoxic effect was achieved with T-DM1. *In vivo*, trastuzumab-dolaflexin yielded marked antitumor activity in the N87 HER2-amplified xenograft model at 10%–30% of the antibody equivalent doses that were required for T-DM1 activity.

Bystander capability of a payload is also an important consideration for efficacy and tolerability (12, 13). Generally, payloads capable of bystander effect are considered more efficacious, particularly in tumors with heterogeneous antigen expression, but these payloads are also less well-tolerated. In contrast, payloads that are incapable of the bystander effect, due to their lack of membrane permeability, are often better tolerated, but can be less efficacious or lead to less durable responses. Two payloads which have been well characterized for their contrasting properties and abilities to effect bystander killing are the auristatins MMAE and MMAF. MMAE is reported to cause bystander killing of neighboring antigen-negative cells due to its cell permeability and lipophilicity (14). In contrast, MMAF was shown not to cause bystander killing, which has been attributed to its reduced cell permeability associated with its greater hydrophilicity.

The dolaflexin platform provides a "controlled bystander" effect. The released payload AF-HPA has a comparable lipophilicity and cell permeability with that of MMAE, and, like MMAE, is capable of bystander killing. However, metabolism of AF-HPA within the tumor to AF, which has a lipophilicity and cell permeability very similar to that of its close analogue MMAF, results in loss of the ability to passively cross the cell membrane, like MMAF, and thereby loss of bystander killing capability. The lack of cell permeability of AF, together with the finding that it is not actively effluxed by Pgp multi-drug resistance pumps, can contribute to accumulation and retention of AF in tumors, consistent with increased activity observed in resistant models with a dolaflexin ADC relative to T-DM1 reported elsewhere (15). In addition, because of its reduced cell permeability, free AF in plasma is less able to enter healthy cells, which may account for the lack of neutropenia observed with the dolaflexin ADC.

The dolaflexin platform represents a novel approach toward ADCs with distinct advantages. The highly hydrophilic fleximer polymer provides a means to compensate for the high hydrophobicity of the auristatin payload, allowing for the preparation of ADCs with

significantly higher DAR without sacrificing physicochemical and pharmacokinetic properties. In turn, the more highly loaded ADCs provide more efficient delivery of the cytotoxic payload to tumor cells, thereby improving efficacy relative to conventional ADCs with a DAR of 3–4, particularly in low antigen–expressing tumors. Despite the higher DAR and increased potency of the dolaflexin ADCs, the controlled bystander effect resulting from the novel AF-HPA payload demonstrates the potential to increase tolerability and eliminate the commonly observed dose-limiting toxicity of neutropenia associated with other bystander-capable auristatin ADC platforms. Clinical evaluation of the dolaflexin platform in the context of XMT-1536, which targets NaPi2b, is ongoing, and results will be published in due course (16).

Authors' Disclosures

A.V. Yurkovetskiy reports contribution to this publication he made during employment at Mersana Therapeutics, which ended 4 years ago in December 2016. N.D. Bodyak reports other from Mersana Therapeutics outside the submitted work. J.D. Thomas reports a patent for US 9,849,191 issued and US 17/024,023 issued. S.M. Clardy reports employment with and is a stockholder of Mersana Therapeutics. M.J. DeVit reports personal fees from Mersana Therapeutics outside the submitted work. P.U. Park reports other from Mersana Therapeutics during the conduct of the study, as well as has a patent for US9808528B2 pending and issued. T.B. Lowinger reports employment with and stockholder of Mersana Therapeutics. No disclosures were reported by the other authors.

Authors' Contributions

A.V. Yurkovetskiy: Conceptualization, formal analysis, methodology, writing–original draft. **N.D. Bodyak:** Conceptualization, data curation, methodology, writing–original draft. **M. Yin:** Conceptualization, investigation, methodology. **J.D. Thomas:** Conceptualization, data curation, methodology. **S.M. Clardy:** Formal analysis, investigation. **P.R. Conlon:** Investigation. **C.A. Stevenson:** Investigation. **A. Uttard:** Investigation. **L. Qin:** Investigation. **D.R. Gumerov:** Investigation. **E. Ter-Ovanesyan:** Investigation. **C. Bu:** Investigation. **A.J. Johnson:** Investigation. **V.R. Gurijala:** Investigation. **D. McGillicuddy:** Investigation. **M.J. DeVit:** Investigation. **L.L. Poling:** Investigation. **M. Protopopova:** Investigation. **L. Xu:** Investigation, methodology. **Q. Zhang:** Investigation. **P.U. Park:** Supervision. **D.A. Bergstrom:** Supervision, writing–original draft. **T.B. Lowinger:** Conceptualization, formal analysis, supervision, investigation, methodology, writing–original draft, project administration, writing–review and editing.

Acknowledgments

The authors gratefully acknowledge the assistance of Drs. Marc Damelin, Eric Hailman, Radha Iyengar, David Lee, and Rebecca Mosher. The authors also thank Theresa E. Singleton for proofreading the article and offering valuable suggestions, which was funded by Mersana Therapeutics in accordance with Good Publication Practice (GPP3) guidelines.

The costs of publication of this article were defrayed in part by the payment of page charges. This article must therefore be hereby marked *advertisement* in accordance with 18 U.S.C. Section 1734 solely to indicate this fact.

Received March 24, 2020; revised August 4, 2020; accepted March 10, 2021; published first March 15, 2021.

References

1. Tolcher AW. The evolution of antibody-drug conjugates: A positive inflexion point. Am Soc Clin Onc Educational Book 2020;40:127–34.
2. Peters C, Brown S. Antibody-drug conjugates as novel anti-cancer chemotherapeutics. Biosci Rep 2015;35:e00225.
3. Diamantis N, Banerji U. Antibody-drug conjugates–an emerging class of cancer treatment. Br J Cancer 2016;114:362–7.
4. Sun X, Ponte JF, Yoder NC, Laleau R, Coccia J, Lanieri L, et al. Effects of drug-antibody ratio on pharmacokinetics, biodistribution, efficacy, and tolerability of antibody-maytansinoid conjugates. Bioconjug Chem 2017; 28:1371–81.
5. Hamblett KJ, Senter PD, Chace DF, Sun MMC, Lenox J, Cerveny CG, et al. Effects of drug loading on the antitumor activity of a monoclonal antibody drug conjugate. Clin Cancer Res 2004;10:7063–70.
6. Saber H, Leighton JK. An FDA oncology analysis of antibody-drug conjugates. Regul Toxicol Pharmacol 2015;71:444–52.
7. Pettit GR, Kamano Y, Herald CL, Tuinman AA, Boettner FE, Kizu H, et al. The isolation and structure of a remarkable marine animal antineoplastic constituent: dolastatin 10. J Am Chem Soc 1987;109:6883–5.
8. Barok M, Tanner M, Köninki K, Isola J. Trastuzumab-DM1 causes tumour growth inhibition by mitotic catastrophe in trastuzumab-resistant breast cancer cells *in vivo*. Breast Cancer Res 2011;13:R46.
9. Yurkovetskiy AV, Yin M, Bodyak N, Stevenson CA, Thomas JD, Hammond CE, et al. A polymer-based antibody-vinca drug conjugate platform: characterization and preclinical efficacy. Cancer Res 2015;75:3365–72.
10. Pettit GR, Srirangam JK, Barkoczy J, Williams MD, Boyd MR, Hamel E, et al. Antineoplastic agents 365. Dolastatin 10 SAR probes. Anticancer Drug Des 1998; 13:243–77.
11. Lyon RP, Bovee TD, Doronina SO, Burke PJ, Hunter JH, Neff-LaFord HD, et al. Reducing hydrophobicity of homogeneous antibody-drug conjugates improves pharmacokinetics and therapeutic index. Nat Biotechnol 2015;33: 733–5.
12. Kovtun YV, Audette CA, Ye Y, Xie H, Ruberti MF, Phinney SJ, et al. Antibody-drug conjugates designed to eradicate tumors with homogeneous and heterogeneous expression of the target antigen. Cancer Res 2006;66: 3214–21.
13. Polson AG, Calemine-Fenaux J, Chan P, Chang W, Christensen E, Clark S, et al. Antibody-drug conjugates for the treatment of non-Hodgkin's lymphoma: target and linker-drug selection. Cancer Res 2009;69:2358–64.
14. Li F, Emmerton KK, Jonas M, Zhang X, Miyamoto JB, Setter JR, et al. Intracellular released payload influences potency and bystander-killing effects of antibody-drug conjugates in preclinical models. Cancer Res 2016;76:2710–9.
15. Le Joncour V, Martins A, Puhka M, Isola J, Salmikangas M, Laakkonen P, et al. A novel anti-HER2 antibody-drug conjugate XMT-1522 for HER2-positive breast and gastric cancers resistant to trastuzumab emtansine. Mol Cancer Ther 2019; 18:1721–30.
16. Bodyak ND, Mosher R, Yurkovetskiy AV, Yin M, Bu C, Conlon PR, et al. The dolaflexin-based antibody-drug conjugate XMT-1536 targets the solid tumor lineage antigen SLC34A2/NaPi2b. Mol Cancer Ther 2021;20:896–905.